Fragment Ion Formation in Resonance Enhanced Multiphoton Ionization (REMPI) of *n*-Propyl Phenyl Ether in a Supersonic Jet

Kyuseok Song,[†] Alexander van Eijk,[‡] Thomas A. Shaler,[§] and Thomas Hellman Morton*
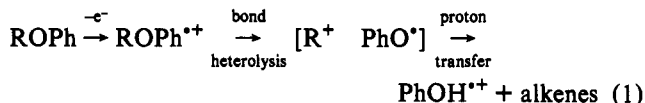
Contribution from the Department of Chemistry, University of California, Riverside, California 92521-0403

Received September 27, 1993. Revised Manuscript Received January 18, 1994[⊗]

Abstract: Resonance enhanced multiphoton ionization (REMPI) mass spectra of different conformational isomers of *n*-propyl phenyl ether at 30 K give the same fragmentation patterns. Laser REMPI excitation spectra exhibit three principal conformers in a supersonic free jet expansion. The most abundant species in the jet happens also to contribute the longest wavelength 0,0 band. SCF calculations suggest that the lowest energy structure corresponds to a *gauche* geometry in which all the carbons except that of the methyl group are essentially coplanar with the oxygen. This is confirmed by experimental observation of a predicted blue shift for a prominent vibrational overtone when the propyl group is partially deuterated (β,β-d_2 or $\alpha,\alpha,\gamma,\gamma,\gamma$-$d_5$). Time-of-flight mass spectra of deuterated analogues of each of three conformers exhibits propene expulsion to yield PhOH$^{\bullet+}$ and PhOD$^{\bullet+}$ (the principal fragment ions) in which all seven alkyl hydrogens have become randomized within the chain. REMPI of individual conformers (*via* intermediacy of the lowest vibrational levels of their excited singlet electronic states) therefore gives the same outcome as does field ionization or electron impact source mass spectra. The predominant decomposition mechanism of the radical cation involves an ion–neutral complex, *n*PrOPh$^{\bullet+}$ → [*i*Pr$^+$ PhO$^{\bullet}$], in which the hydrogens of the *i*Pr$^+$ undergo rapid internal transpositions prior to the ultimate decomposition step. *Ab initio* computations on a model system concur with the experimental inference that this mechanism operates regardless of the conformation of the precursor neutral.

Resonance enhanced multiphoton ionization (REMPI) has proven to be an experimental tool of great value in a variety of investigations of molecular spectroscopy.[1] REMPI mass spectrometry (also known as mass resolved excitation spectroscopy) using a supersonic free jet expansion has, in particular, been demonstrated as a powerful method for examining structures and electronic and vibronic states of isolated molecules containing aromatic[1,2] and linear[3,4] π-systems. It has been used, for example, to prove the conformations of flexible substituents attached to a benzene ring.[5,6] By means of this technique Bernstein and co-

workers determined that anisole has only one low-lying conformer and that its methoxy group lies in the same plane as the benzene ring,[5] while laser-induced fluorescence studies show that propyl-substituted benzene rings have more than one conformer due to the longer chain length of the substituent.[7–9] Therefore *n*-propyl phenyl ether (*n*PrOPh) is expected to have at least two low-lying conformational isomers. In a supersonic jet these can be studied by REMPI, since interconversion between stable conformers ought to be frozen out, and each can thus be independently excited by a laser source. The present study explores the REMPI of jet-cooled *n*PrOPh using single-wavelength nanosecond pulses. Our conclusion is that the radical cation formed by REMPI decomposes by the pathway represented in eq 1, regardless of the conformation of the neutral precursor ROPh.

$$ \text{ROPh} \xrightarrow{-e^-} \text{ROPh}^{\bullet+} \xrightarrow[\text{heterolysis}]{\text{bond}} [\text{R}^+ \ \text{PhO}^{\bullet}] \xrightarrow{\text{proton transfer}} $$

$$ \text{PhOH}^{\bullet+} + \text{alkenes} \quad (1) $$

Propyl phenyl ether warrants scrutiny in this regard because of the important role its positive ions have played in elucidating

† Present address: Korea Atomic Energy Research Institute, P.O. Box 7, Taedok Science Town, Taejon, Korea.
‡ Present address: Voordorp 71, 2352 BV Leiderdarp, The Netherlands.
§ Present address: SRI International, Molecular Physics Laboratory, 333 Ravenswood Avenue, Menlo Park, CA 94025.
⊗ Abstract published in *Advance ACS Abstracts,* April 1, 1994.
(1) (a) Boesl, U.; Weinkauf, R.; Walter, K.; Weickhardt, C.; Schlag, E. W. *J. Phys. Chem.* **1990**, *94*, 8567–8573. (b) Neusser, H. J. *J. Phys. Chem.* **1989**, *93*, 3897–3907, and references therein.
(2) (a) Dunn, T. M.; Tembruell, R.; Lubman, D. M. *Chem. Phys. Lett.* **1985**, *121*, 453–457. (b) Tubergen, M. J.; Cable, J. R.; Levy, D. H. *J. Chem. Phys.* **1990**, *92*, 51–60. (c) Hiraya, A.; Achiba, Y.; Kimura, K.; Lim, E. C. *Chem. Phys. Lett.* **1991**, *185*, 303–309. (d) Cockett, M. C. R.; Takahashi, M.; Okuyama, K.; Kimura, K. *Chem. Phys. Lett.* **1991**, *187*, 250–256. (e) Weber, T.; Riedle, E.; Neusser, J. H.; Schlag, E. W. *Chem. Phys. Lett.* **1991**, *183*, 77–83. (f) Bernstein, E. R. *J. Phys. Chem.* **1992**, *96*, 10 105–10 115. (g) Philis, J. G. *J. Mol. Spectrosc.* **1992**, *152*, 441–444. (h) Philis, J. G. *J. Mol. Spectrosc.* **1992**, *155*, 215–216. (i) Disselkamp, R.; Bernstein, E. R.; Seeman, J. I.; Secor, H. V. *J. Chem. Phys.* **1992**, *97*, 8130–8136. (j) Dyke, J. M.; Ozeki, H.; Takahashi, M.; Cockett, M. C. R.; Kimura, K. *J. Chem. Phys.* **1992**, *97*, 8926–8933. (k) Kosmidis, C.; Bolovinos, A.; Tsekeris, P. *J. Mol. Spectrosc.* **1993**, *160*, 186–191. (l) Steenvoorden, R. J. J. M.; Vasconcelos, M. H.; Kistemaker, P. G.; Weeding, T. L. *J. Mol. Spectrosc.* **1993**, *161*, 17–27. (m) Zinger, E.; Haas, Y. *Chem. Phys. Lett.* **1993**, *202*, 442–451. (n) Saigusa, H.; Lim, E. C. *Chem. Phys. Lett.* **1993**, *211*, 410–415. (o) Reiser, G.; Rieger, D.; Wright, T. G.; Müller-Dethlefs, K.; Schlag, E. W. *J. Phys. Chem.* **1993**, *97*, 4335–4343. (p) Finley, J. P.; Cable, J. R. *J. Phys. Chem.* **1993**, *97*, 4595–4600. (q) Weersink, R. A.; Wallace, S. C. *J. Phys. Chem.* **1993**, *97*, 6127–6133. (r) Disselkamp, R.; Bernstein, E. R. *J. Chem. Phys.* **1993**, *98*, 4339–4354. (s) Barstis, T. L. O.; Grace, L. I.; Dunn, T. M.; Lubman, D. M. *J. Phys. Chem.* **1993**, *97*, 5820–5825.
(3) (a) Buma, W. J.; Kohler, B. E.; Song, K. *J. Chem. Phys.* **1990**, *92*, 4622–4623. (b) Buma, W. J.; Kohler, B. E.; Song, K. *J. Chem. Phys.* **1991**, *94*, 6367–6376. (c) Buma, W. J.; Kohler, B. E.; Song, K. *J. Chem. Phys.* **1991**, *94*, 4691–4698. (d) Buma, W. J.; Kohler, B. E.; Shaler, T. A. *J. Chem.*

Phys. **1992**, *96*, 399–407. (e) Sabljic, A.; McDiarmid, R.; Gedanken, A. *J. Phys. Chem.* **1992**, *96*, 2442–2448. (f) Buma, W. J.; Kohler, B. E.; Nuss, J. M.; Shaler, T. A.; Song, K. *J. Chem. Phys.* **1992**, *96*, 4860–4868. (g) Ci, X.; Kohler, B. E.; Moller, S.; Shaler, T. A.; Yee, W. A. *J. Phys. Chem.* **1993**, *97*, 1515–1520.
(4) (a) Minsek, D. W.; Blush, J. A.; Chen, P. *J. Chem. Phys.* **1992**, *96*, 2025–2029; **1993**, *97*, 8675. (b) Blush, J. A.; Minsek, D. W.; Chen, P. *J. Phys. Chem.* **1992**, *96*, 10150–10154. (c) Williams, B. A.; Cool, T. A. *J. Phys. Chem.* **1993**, *97*, 1270–1282.
(5) Breen, P. J.; Bernstein, E. R.; Secor, H. V.; Seeman, J. I. *J. Am. Chem. Soc.* **1989**, *111*, 1958–1968.
(6) (a) Li, S.; Bernstein, E. R.; Seeman, J. I. *J. Phys. Chem.* **1992**, *96*, 8808–8813 and references contained therein. (b) Disselkamp, R.; Im, H. S.; Bernstein, E. R. *J. Chem. Phys.* **1992**, *97*, 7889–7901.
(7) (a) Hopkins, J. B.; Powers, D. E.; Smalley, R. E. *J. Chem. Phys.* **1980**, *72*, 5039–5048. (b) Hopkins, J. B.; Powers, D. E.; Mukamel, S.; Smalley, R. E. *J. Chem. Phys.* **1980**, *72*, 5049–5061.
(8) Song, K.; Hayes, J. M. *J. Mol. Spectrosc.* **1989**, *134*, 82–97.
(9) (a) Martinez, S. J. III; Alfano, J. C.; Levy, D. H. *J. Mol. Spectrosc.* **1989**, *137*, 420–426. (b) Martinez, S. J. III; Alfano, J. C.; Levy, D. H. *J. Mol. Spectrosc.* **1993**, *158*, 82–92.

4456 *J. Am. Chem. Soc., Vol. 116, No. 10, 1994*

Song et al.

new gas-phase decomposition pathways.[10] Alkyl phenyl ethers continue to be widely studied as examples of compounds whose molecular ions decompose *via* ion–neutral complexes, as represented in eq 1, in which the final products are formed by a proton transfer from an alkyl cation to a phenoxy radical that are in orbit around one another.[11-15] Although this may not be the exclusive pathway by which all alkyl phenyl ether molecular ions (ROPh·+) expel alkenes,[13] there is abundant evidence that it is the predominant pathway for alkene expulsion when R is a primary alkyl group larger than ethyl. Chronister and Morton examined *n*-propyl phenyl ethers (PhOCH$_2$CH$_2$CH$_3$ = *n*PrOPh-*d*$_0$, PhOCH$_2$CD$_2$CH$_3$ = *n*PrOPh-β-*d*$_2$, PhOCD$_2$CH$_2$CD$_3$ = *n*PrOPh-α,γ-*d*$_5$) using two-color (266 and 532 nm) REMPI with picosecond pulses and demonstrated that ion–neutral complexes are intermediates when M·+ ions of these molecules decompose.[12] Since those studies were performed with samples at room temperature, the internal energy of ions in relation to the real intermediate states (S$_1$) of the parent neutral was not well determined. The present study shows that the same mechanism operates when individual conformers are ionized in a one-color REMPI experiment, where the intermediate excited neutral is the vibrational ground state of S$_1$. Therefore any conformational interconversion must take place after absorption of a second photon, which brings the electronic energy of the system to a state above the ionization energy of the neutral precursor.

Decomposition patterns of ionized species are measured using time of flight (TOF) mass spectrometry. The widths of the individual TOF peaks correspond to the laser pulsewidth, 10^{-8} s. When REMPI-TOF mass spectrometry makes use of 0,0-transitions of neutral molecules, the mass spectrum reflects the formation and fragmentation of ions from conformationally frozen neutrals on the 0.01 μs time scale.

Experimental Section

n-Propyl phenyl ether (*n*PrOPh-*d*$_0$) was prepared by reaction of 1-iodopropane (Aldrich) with sodium phenoxide in THF and purified by washing with 20% aqueous NaOH followed by distillation, bp 187–189 °C, n$_D$^{20} 1.5008; bp (lit.)[16] 189.3 °C, or was synthesized by lithium aluminum hydride reduction of 3-bromopropyl phenyl ether (Aldrich). Isotopic analogues of *n*-propyl phenyl ether (*n*PrOPh-β-*d*$_2$ and *n*PrOPh-α,γ-*d*$_5$) were prepared as previously described.[12] In our experiments a molecular beam made by a free jet expansion of propyl phenyl ether seeded into helium was intersected at right angles by the focused beam of the excitation laser in an apparatus that has been described elsewhere.[3a-d] Ions formed at this intersection point were accelerated along the third orthogonal direction into a time of flight (TOF) mass spectrometer. The resonance enhanced excitation spectrum consists of a plot of the average number of ions at a particular charge-to-mass ratio (*m*/*z*) versus laser wavelength. The mass resolution, defined as $R = T/2\Delta T$ where T is the total flight time of the ion packet and ΔT is the FWHM of the peak,[17] had a value, $R = 17 \times 10^3$ ns/15 ns = 1133.

(10) (a) Benoit, F. M.; Harrison, A. G. *Org. Mass. Spectrom.* **1976**, *11*, 599–608. (b) Borchers, F.; Levsen, K.; Beckey, H. D. *Int. J. Mass Spectrom. Ion Phys.* **1976**, *21*, 125–132.

(11) (a) McAdoo, D. J.; Morton, T. H. *Acc. Chem. Res.* **1993**, *26*, 295–302. (b) Morton, T. H. *Org. Mass Spectrom.* **1992**, *27* 353–368. (c) Longevialle, P. *Mass Spectrom. Rev.* **1992**, *11*, 157–192. (d) Bowen, R. C. *Acc. Chem. Res.* **1991**, *24*, 364–371. (e) Hammerum, S. In *Fundamentals of Gas Phase Ion Chemistry*; Jennings, K. R., Ed.; Kluwer Academic Publishers: Dordrecht, 1990; pp 379–390. (f) McAdoo, D. J. *Mass Spectrom. Rev.* **1988**, *7*, 363–393. (g) Morton, T. H. *Tetrahedron* **1982**, *38*, 3195–3243. (h) Morton, T. H. *J. Am. Chem. Soc.* **1980**, *102*, 1596–1602. (i) Bowen, R. D.; Williams, D. H.; Schwarz, H. *Angew. Chem., Int. Ed. Engl.* **1979**, *18*, 451–461.

(12) Chronister, E. L.; Morton, T. H. *J. Am. Chem. Soc.* **1990**, *112*, 133–139.

(13) (a) Sozzi, G.; Audier, H. E.; Mourgues, P.; Millet, A. *Org. Mass Spectrom.* **1987**, *22*, 746–747. (b) Kondrat, R. W.; Morton, T. H. *Org. Mass Spectrom.* **1988**, *23*, 555–557.

(14) (a) Blanchette, M. C.; Holmes, J. L.; Lossing, F. P. *Organic Mass Spectrom.* **1989**, *24*, 673–678. (b) Harnish, D.; Holmes, J. L. *J. Am. Chem. Soc.* **1991**, *113*, 9729–9734.

(15) Nguyen, V.; Cheng, X.; Morton, T. H. *J. Am. Chem. Soc.* **1992**, *114*, 7127–7132, and references contained therein.

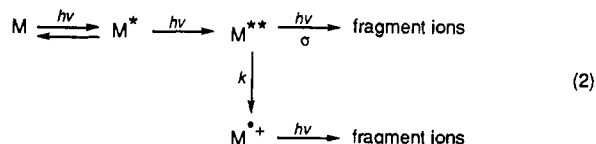(16) Perkin, W. H., Jr. *J. Chem. Soc.* **1896**, *69*, 1025.

(17) Lubman, D. M.; Jordan, R. M. *Rev. Sci. Instrum.* **1985**, *56*, 373–375.

The excitation source was the frequency-doubled output of a dye laser (Spectra Physics model PDL-2) pumped by a Nd:YAG laser (Spectra Physics Model DCR-3). Two types of spatial profiles were used in these experiments: one in which the pump laser operates as an unstable resonator ("doughnut mode") and one (using a different rod) in which the transverse beam profile is nearly Gaussian. The former is produced in a resonator that has a high magnification factor resulting from an output coupler with a highly reflective dot at its center (DCR-3D). A pseudo-Gaussian beam is produced by an output coupler that is partially reflective over its entire convex surface with a lower magnification (DCR-3G) resonator. Unless otherwise indicated the laser-jet studies described here were run in doughnut mode. The dye laser used Coumarin 500, Coumarin 540A, and Fluorescein 548 (Exciton). Coumarin 500 and Coumarin 540A were pumped by the third harmonic of the Nd:YAG laser (355 nm), while Fluorescein 548 was pumped by the second harmonic (532 nm). Frequency doubling of the dye fundamental was performed using a Spectra Physics Model WEX-1 wavelength extender. Ultraviolet light from the WEX-1 was focused by a 20-cm focal length convex lens (spot diameter on the order of 2 × 10^{-5} m) into the excitation region in the vacuum chamber at a right angle to the molecular beam. For power dependence studies, the laser power was measured by a Laser Precision Rj 7200 energy meter with an RTP 735 detector head. The energy of the laser was averaged 300–500 shots to minimize energy fluctuation of the laser.

SCF calculations were performed using the SPARTAN software (Version 3.0, which includes animation of normal modes and computes the effects of deuterium substitution) on a Silicon Graphics 4D/35 Personal Iris computer[18] or using GAUSSIAN[19] on the Cray YMP 8/864 at the San Diego Supercomputing Center. Except for the transition state drawn in Figure 3, all geometries were located using Berny optimization.[20] Basis set superposition errors (BSSE) were estimated using the counterpoise method.[21] This correction was made for all SCF computations on C$_3$H$_7$-NH$_3$+ geometries.

Results

The process by which REMPI operates in these experiments is generalized in eq 2. The resonant process corresponds to the absorption of the first photon, which results in promotion of the neutral to its lowest excited singlet (S$_1$) state, represented here as M*. Absorption of subsequent photons by M* leads to ionization to M·+ and fragmentation. From the similarities between the spectra reported here and those previously published by Chronister and Morton[12] we conclude that observed charged fragments are produced by decompositions of M·+, not by fragmentation of the neutral followed by ionization of the fragments. Experiments below document the effects of varying the excitation wavelength on the M·+ yield (at a laser power where that is virtually the only ion observed) and the variation of the fragment spectrum as a function of both wavelength and laser power.

$$M \underset{}{\overset{h\nu}{\rightleftharpoons}} M^* \xrightarrow{h\nu} M^{**} \xrightarrow[\sigma]{h\nu} \text{fragment ions}$$

$$\downarrow k$$

$$M^{\cdot+} \xrightarrow{h\nu} \text{fragment ions} \qquad (2)$$

Spectra and Vibrational Analysis. Figure 1 shows the REMPI excitation spectra of *n*PrOPh-*d*$_0$, -β-*d*$_2$, and -α,γ-*d*$_5$ over a 1000-cm^{-1} domain. The most intense feature occurs at the lowest energy of each spectrum (36 345 cm^{-1}) and is marked as **a**. Band **a** occurs at the same frequency (±1 cm^{-1}) for all three isotopic variants and is assigned as the origin band of the S$_0$ → S$_1$ transition

(18) SPARTAN, Wavefunction Inc., Irvine, CA. For the optimization method used to determine transition state geometry in Figure 3, see: Baker, J.; Hehre, W. J. *J. Comput. Chem.* **1991**, *12*, 606–610.

(19) GAUSSIAN 92, Revision B; Frisch, M. J.; Trucks, G. W.; Head-Gordon, M.; Gill, P. M. W.; Wong, M. W.; Foresman, J. B.; Johnson, B. G.; Schlegel, H. B.; Robb, M. A.; Replogle, E. S.; Gomperts, R.; Andres, J. L.; Raghavachari, K.; Binkley, J. S.; Stewart, J. J. P.; Pople, J. A. Gaussian, Inc.: Pittsburgh, PA.

(20) Schlegel, H. B. *J. Chem. Phys.* **1982**, *77*, 3676–3681.

(21) Latajka, Z.; Scheiner, S.; Chalesinski, G. *Chem. Phys. Lett.* **1992**, *196*, 384–389.

REMPI of n-Propyl Phenyl Ether

J. Am. Chem. Soc., Vol. 116, No. 10, 1994   4457
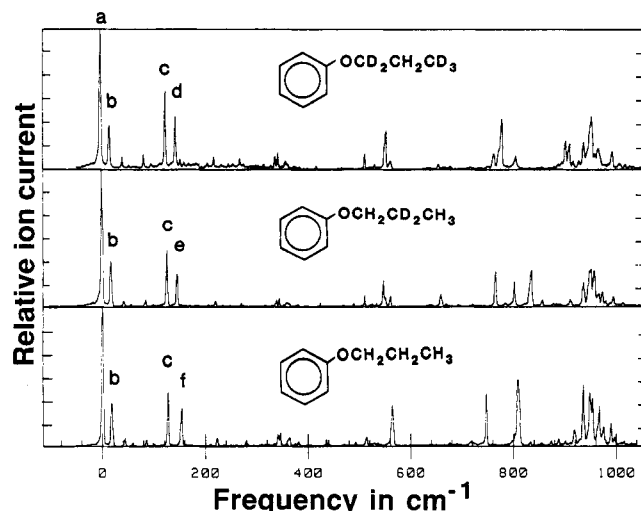
Figure 1. Excitation spectra (ion current versus laser frequency relative to the origin band at 36 345 cm⁻¹) of n-propyl phenyl ethers monitored by TOF mass spectroscopy.

Table 1. Vibrational Analysis of n-Propyl Phenyl Ethers (nPrOPh) in cm⁻¹ [a]

| mode | d_0 | | | |
	S_0 (liquid)	S_1	S_1	S_1
T_1		42	42	40
$T2$		153 (f)	146 (e)	152 (d)
$T3$		258	250	262
16a	411	340	339	334
$T4$		345	344	340
16b	512	434	425	415
6a′	616	513	512	510
6b		563	547	550
6a″	787	747	768	776
10a	810	808	802	803

[a] The numbering system for stretching and bending modes (in italics) is based on that for the vibrational spectrum of benzene.[22] Vibrational modes assigned to the side chain are designated as T1–T4. One ring mode extensively coupled to side chain motions is split into vibrations 6a′ and 6a″.

for the major conformer of each molecule. Since this is the most intense band, the equilibrium geometry of the excited state is probably not much different from that of the ground state. Most of the low intensity bands <350 cm⁻¹ from the origin band can be assigned as vibrational modes of the propoxy group. Among these low-frequency bands, however, two (17 and 126 cm⁻¹ to the blue of the origin band) occur at the same frequency (within 0.1 cm⁻¹) in all three spectra (marked as **b** and **c** in Figure 1). If these were vibrational modes of the S₁ state there should have been some frequency shift as a consequence of deuterating the substituent (as we calculate *ab initio* for all the vibrational frequencies below 400 cm⁻¹ in S₀). Such a shift is seen, for example, in the bands labeled **d**, **e**, and **f**. Since no frqeuency shift upon deuteration was observed for bands **a**, **b**, or **c**, the latter two bands are assigned as origin bands of other conformational isomers. There is also a weak band 221 cm⁻¹ to the blue of the origin band in the d_0 and d_2 compounds, a region that is obscured in the excitation spectrum of the d_5. This may represent yet another conformational isomer.

The REMPI excitation spectrum of nPrOPh is interpreted as the superposition of three major conformers with possibly a minor contribution from a fourth. Two rotamers have been reported in the case of n-butylbenzene,[7] which can be viewed as an analogue to nPrOPh, in which the oxygen is replaced by a methyl group. The case of nPrOPh appears to be more complicated. In the present study we infer a vibrational temperature on the order of 30 K for molecules within the jet by means of experiments in which a trace of aniline was added. The temperature was calculated by taking the intensity ratio of the I_1^1 band ($\Delta\nu = 292$ cm⁻¹) and the 0,0 band of aniline. It is therefore consistent with previous studies to infer that individual conformers do not interconvert on the excitation time scale, but we cannot ascertain whether their distribution corresponds to the equilibrium at the helium bath temperature, the jet temperature, or some intermediate distribution.

With the supposition that nPrOPh has three major low-lying conformational isomers we can assign most of the bands <900 cm⁻¹ from the origin in Figure 1, as Table 1 summarizes (using the numbering system for the vibrations of benzene[22]). Band assignments for ring modes are based on comparisons with alkylbenzenes, phenol, anisole, and phenetole[22–24] as well as the SCF normal modes computed at 3-21G for the electronic ground

states. As can be seen by the comparison between our experimental results for the ground and excited states of the undeuterated analogue in Table 1, there are large differences between the vibrational frequencies for S₀ in the liquid phase and those for S₁ in the jet. We do not attempt to assign side-chain vibrations on the basis of our calculations of ground-state vibrational structure, since C–O bond lengths become substantially shorter in the excited state and torsional barriers increase for substituents bonded to the benzene ring.[24] Although REMPI excitation spectra of nPrOPh (d_0, β-d_2, α,γ-d_5) were measured down to wavelengths in the 260-nm region, complete assignment of bands >900 cm⁻¹ from the origin is difficult because of spectral congestion. In addition, other excited electronic states may be present at higher energies.

Conformational Analysis. Assignment of conformations corresponding to bands **a** and **b** is based on *ab initio* calculations. The conventional terms *anti* and *gauche* will be used to designate rotamers about sp³–sp³ C–C bonds. In the present context *anti* designates a dihedral angle between C–O and C–CH₃ bonds close to 180° and *gauche* designates a dihedral angle near 60°. We have performed SCF calculations on a half-dozen stable geometries using the 3-21G basis set. Previous computations at this level have provided a description of *gauche* and *anti* conformers of FCH₂CH₂OPh that agrees well with observed NMR coupling constants.[15] In that work the *gauche* was found to be favored energetically, in keeping with the known properties of β-fluorosubstituted, acyclic systems. In the present case, *ab initio* calculations also predict a *gauche* structure to have a lower energy than any of the *anti* rotamers, in a fashion consistent with earlier predictions for n-propanol[25] and its methyl ether.[26] Three *anti* and three *gauche* geometries have been examined.

The *anti* conformer with the lowest electronic energy has all of its carbons coplanar with the oxygen. This structure, which has C_s symmetry (although that was not imposed as a constraint), will here be called "planar *anti*." While this is the most favorable conformation predicted by molecular mechanics (MM2), at 3-21G the corresponding *gauche* rotamer has a lower electronic energy and is calculated to be more stable by 1.8 kJ mol⁻¹ (0.45 kcal mol⁻¹) when zero point vibrational energies are taken into

(22) (a) Varsanyi, G. *Vibrational Spectra of Benzene Derivatives*; Academic Press: New York and London, 1969; pp 71, 141–339. (b) Gruner, D.; Brumer, P. *J. Chem. Phys.* **1991**, *94*, 2848–2861. (c) Takahashi, M.; Kimura, K. *J. Chem. Phys.* **1992**, *97*, 2920–2927.

(23) (a) Balfour, W. J. *J. Mol. Spectrosc.* **1985**, *109*, 60–72. (b) Balfour, W. J. *Spectrochim. Acta* **1983**, *39A*, 795–800. (c) Owen, N. L.; Hester, R. E. *Spectrochim. Acta* **1969**, *25A*, 343–354. (d) Murray, M. J.; Cleveland, F. F. *J. Chem. Phys.* **1941**, *9*, 129–132. (e) Bist, H. D.; Brand, J. C. D.; Williams, D. R. *J. Mol. Spectrosc.* **1969**, *24*, 402–12, 413–467. (f) Green, J. H. S. *Spectrochim. Acta* **1962**, *18*, 39–50.

(24) (a) Martinez, S. J. III; Alfano, J. C.; Levy, D. H. *J. Mol. Spectrosc.* **1992**, *152*, 80–88. (b) Takazawa, K.; Fujii, M.; Ito, M. *J. Chem. Phys.* **1993**, *99*, 3205–3217.

(25) Houk, K. N.; Eksterowicz, J. E.; Wu, Y-D.; Fuglesang, C. D.; Mitchell, D. B. *J. Am. Chem. Soc.* **1993**, *115*, 4170–4177.

(26) Wiberg, K. B.; Murcko, M. A. *J. Am. Chem. Soc.* **1989**, *111*, 4821–4828.
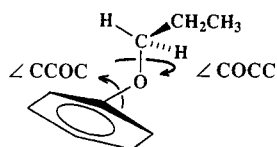
Figure 2. Pertinent angles for describing C–O bond rotamers of *n*-propyl phenyl ether. Depicted is a [90,180] geometry, in which ∠CCOC ≅ 90° and ∠COCC ≅ 180°.

Table 2. Relative SCF Electronic Energies for Conformational Isomers of *n*-Propyl Phenyl Ether (3-21G//3-21G)

conformer	∠CCOC (deg)	∠COCC (deg)	E_{el} (3-21G) (kJ mol^{-1})
[0, 180] *gauche*	0	179	0
planar *anti* ([0, 180])	0	180	2.4
[0, 90] *gauche*	3	81	4.9
[90, 180] *gauche*	92	177	5.5
chiral *anti* ([0, 90])	2	82	7.3
perpendicular *anti* ([90, 180])	90	180	8.5

consideration. These structures are depicted by the Newman projections drawn below.

planar *anti* ([0,180])   [0,180] *gauche*
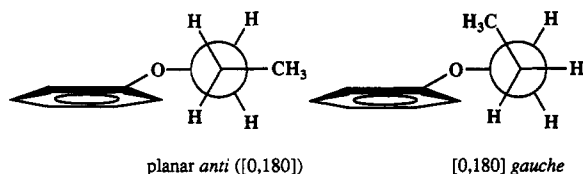
Conformational isomerism about the carbon–oxygen bonds will be designated by two dihedral angles, ∠CCOC and ∠COCC, as portrayed in Figure 2. Thus the two lowest energy structures both correspond to [0,180] geometries. Figure 2 depicts the [90,-180] geometries. The [90,180] *anti* is the least stable of the rotamers examined. Its geometry corresponds to the published *anti* structure of FCH$_2$CH$_2$OPh,[15] in which the fluorine has been replaced by a methyl. This rotamer has a mirror plane of symmetry, which is perpendicular to the benzene ring, and it will be designated as the "perpendicular *anti*". The [90,180] *gauche* is calculated to be higher than the [0,180] *gauche* by 4 kJ mol^{-1} when zero point vibrational energies are taken into consideration. The entropy difference mitigates this gap somewhat, and the calculated free energy difference favors the [0,180] *gauche* by only $\Delta G = 1.5$ kJ mol^{-1} at 300 K relative to the [90,180] *gauche*. The remaining stable structures are represented by the sawhorse projections drawn below. Table 2 summarizes the electronic energy differences.

chiral *anti* ([0,90])   [0,90] *gauche*
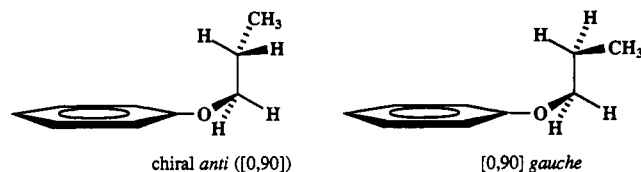
A pair of structures may loosely be designated as [0,90] geometries (if we round off torsional angles to the nearest quadrant). The [0,90] *gauche* corresponds roughly to the most favorable geometry calculated for FCH$_2$CH$_2$OPh (where the corresponding dihedral angles are 37° and 97°).[15] SCF calculations favor the [90,180] *gauche* over the [0,90] *gauche* by 1 kJ mol^{-1} when zero point energies are taken into consideration. The *anti* [0,90] rotamer is chiral, which distinguishes it from the other two *anti* conformers, and we refer to it as the "chiral *anti*" conformation. If we accept the ordering of relative enthalpies from the *ab initio* calculations, bands **a** and **b** in Figure 1 correspond to the [0,180] geometries. Since the planar *anti* is not chiral, the $T\Delta S$ term in the free energy difference between

the two [0,180] conformers is dominated by the contribution from entropy of mixing and favors the *gauche* by 1 kJ mol^{-1} at 300 K in addition to the 2 kJ mol^{-1} enthalpy difference. Band **c** corresponds to one of the other *gauche* conformers and the weak band 221 cm^{-1} to the blue of **a** (if it does represent another conformer) to a third *gauche* conformer.

The SCF-calculated isotopic shifts suggest that band **a** does indeed correspond to a *gauche* isomer. Since the 0,0 bands appear as the most intense peaks in the REMPI excitation spectra, the effects of deuterium substitution on the vibrations of the ground electronic state should be comparable to those for S$_1$. With the aid of computer animation we find that the only low-frequency ring modes that should be substantially affected by isotopic substitution of the side chain are the radial skeletal deformations *1* and *6a*. These two modes are well known to be sensitive to substituents, and *6a* is coupled to motions of the side chain. Therefore there are two normal coordinates that have the character of *6a*, which we shall designate as *6a'* and *6a"*. For the lowest energy *anti* conformation ([0,180]) partial deuteration of the propyl group lowers both of these frequencies slightly (on the order of 4–6 cm^{-1}). For the lowest energy *gauche* conformation ([0,180]), however, partial deuteration lowers *6a'* but raises the frequency corresponding to *6a"*. The calculated blue shifts for *6a"* in S$_0$ are 26 cm^{-1} for β-d_2 and 39 cm^{-1} for α,γ-d_2, as compared with those observed for S$_1$ summarized in Table 1, 21 and 29 cm^{-1}, respectively. As these are the most intense peaks (outside of the origin bands) in the vibrational progressions of the deuterated analogues, we conclude that they must truly belong to the conformer that gives rise to band **a**. The blue shifts calculated for the [90,180] *gauche* are of much smaller magnitude (8–12 cm^{-1}), while a red shift is predicted for the [0,90] *gauche*. Hence we infer that band **a** corresponds to the [0,180] *gauche*. Since **a** is the most intense band, the [0,180] *gauche* must be the most abundant conformational isomer in the jet.

Pathways of Ion Formation. The yield of ions of a given mass as a function of laser power at a given wavelength can be fit by various kinetic schemes. The scheme that we hypothesize is summarized by eq 2. In this equation k is a first-order rate coefficient, and σ is an absorption cross section (in cm^2 photon^{-1}). A molecule M absorbs the first photon to form excited state M*. If the laser power is sufficiently great, M* absorbs a second photon to access a higher excited state M**. If the electronic energy of M** exceeds the ionization energy, M** ejects an electron to form the molecular ion M$^{\bullet+}$. If the laser power is high enough yet another photon is absorbed. Either M$^{\bullet+}$ or M** can absorb this third photon to yield charged fragments. This represents a more general mechanism than the "ladder-switching" model, which has been cited in studies of smaller molecules,[1] where the third photon is absorbed only by M$^{\bullet+}$. The ladder-switching model corresponds to eq 2 in the limit $k \gg \sigma I$, where I stands for the light intensity in photons cm^{-2} s^{-1}.

Phenol$^{\bullet+}$ isotopic ratios were measured for *n*PrOPh-β_2-d_2 and *n*PrOPh-α,γ-d_5. In the range of laser power densities used for these experiments (≤ 300 J cm^{-2} per pulse) molecular ion (M$^{\bullet+}$), PhOH$^{\bullet+}$, and PhOD$^{\bullet+}$ are the principal peaks seen in the TOF mass spectra. While the energy of two photons in this energy range (9.6 eV) is greater than the thermodynamic barrier to form phenol$^{\bullet+}$ and propene, there is an activation barrier on the order of 1 eV for this fragmentation of M$^{\bullet+}$.[14] Power dependence studies confirm the previous observation that M$^{\bullet+}$ (with no detectable fragmentation) is the only ionic product from two-photon absorption in the range 265–275 nm.[12]

At low laser power absorption of a third photon leads to formation of phenol$^{\bullet+}$ as the predominant fragment ion. Equation 1 represents this pathway by which this fragmentation occurs: ion–neutral complexes containing isopropyl cation and phenoxy radical intervene, as revealed by the proportions of PhOD$^{\bullet+}$ and PhOH$^{\bullet+}$ from the β-d_2 and α,γ-d_5 isotopic analogues. The

Table 3. Fragment Ion Ratios from nPrOPh-α,γ-d_5 and -β-d_2[a]

		d_5		
wavelength	2751.5 Å (a)	2750.1 Å (b)	2742.0 Å (c)	2740.05 Å (d)
$\dfrac{m/z\,95}{m/z\,94} = y$	1.51 (0.28)	1.84 (0.26)	2.02 (0.22)	2.07 (0.26)

		d_2		
wavelength	2751.4 Å (a)	2750.2 Å (b)	2741.9 Å (c)	2740.45 Å (e)
$\dfrac{m/z\,94}{m/z\,95} = x$	2.69 (0.17)	2.96 (0.44)	3.09 (0.40)	2.67 (0.36)
$\sqrt{xy}$	2.0 (0.4)	2.3 (0.5)	2.5 (0.4)	2.4 (0.3)
$\sqrt{x/y}$	1.33	1.27	1.24	1.14

[a] Standard deviations are given in parentheses.

signature of the intermediate ion–neutral complexes is the randomization of isotopic label depicted in eqs 3 and 4.
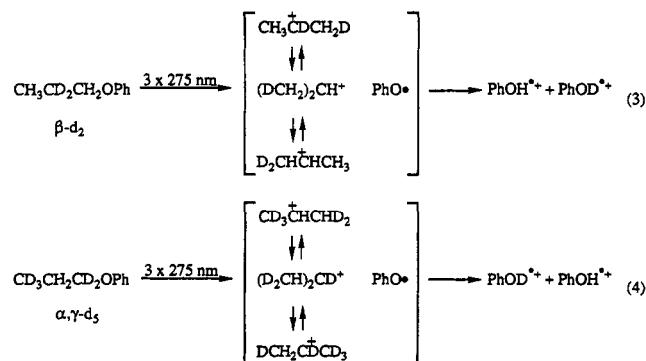
If we call x = the PhOH$^{•+}$/PhOD$^{•+}$ ratio from β-d_2 and y = the PhOD$^{•+}$/PhOH$^{•+}$ ratio from α,γ-d_5, the extent of internal isotopic exchange can be assessed as $\sqrt{xy}$, where a value of 2.5 corresponds to all seven alkyl hydrogens becoming chemically equivalent. As Table 3 summarizes, the experimental values of $\sqrt{xy}$ for all four bands studied are within the 75% confidence limits of this value. The mean primary kinetic isotope effect for the proton-transfer step can be computed as $k_H/k_D = \sqrt{x/y}$. The variation of this value with wavelength is probably not significant.

The results using nanosecond pulses agree very well with the previously reported picosecond data. Small amounts of propyl ions (m/z 43) were observed under the latter conditions (and attributed to absorption of a third photon by M$^{•+}$). In the present study propyl ions could not be detected at laser intensities below 1 mJ per pulse when the pumping laser was operated in doughnut mode. But with a resonator that gives a pseudo-Gaussian spatial profile, however, a small amount of propyl ion can be observed in approximately the same proportion as reported in the picosecond studies.[12] The power threshold for propyl ion in this case is on the order of 50 μJ per pulse. At laser powers >0.2 mJ per pulse, other fragment ions smaller than phenol$^{•+}$ are formed. The first of these to be observed from nPrOPh-d_0 corresponds to $C_5H_6^{•+}$ (m/z 66) that is produced by CO expulsion from phenol$^{•+}$. This result is also seen for β-d_2 and α,γ-d_5 (mutatis mutandis) and is consistent with the picosecond, two-color experiments reported by Chronister and Morton.[12]

Discussion

The radical cation nPrOPh$^{•+}$ decomposes via an intermediate, which renders all seven of the alkyl hydrogens of the propyl group chemically equivalent. Rearrangement of n-propyl (nPr) to isopropyl (iPr) is observed in many gas-phase cations, for example, in the course of the metastable ion decomposition nPrNH$_3^+ \rightarrow$ NH$_4^+$. In that case, only one of the β-hydrogens becomes equivalent with the five α and γ hydrogens (i.e., $\sqrt{xy}$ = 5).[27] In

(27) Audier, H. E.; Morton, T. H. *Org. Mass Spectrom.* **1993**, *28*, 1218–1224.

the present case, however, both β-hydrogens become equivalent with the five α and γ hydrogens (i.e., $\sqrt{xy}$ = 2.5), as Table 3 summarizes. This can be explained either by supposing that the reaction produces a corner-protonated cyclopropane within an ion–neutral complex or else that isopropyl cations are formed within complexes that have enough internal energy for the interconversions drawn in eqs 3 and 4.

Photoionization studies of ethyl phenyl ether (phenetole) have been discussed in terms of six-[28] or four-member[29] cyclic transition states leading to expulsion of ethylene. Mechanisms of this sort cannot be operating in the case of nPrOPh, because (contrary to fact) they predict no participation of α and γ hydrogens (i.e., $\sqrt{xy}$ = zero). Nor can a simple rearrangement from nPrOPh$^{•+}$ to iPrOPh$^{•+}$ account for the results (unless that rearrangement is reversible), since subsequent expulsion of propene via a cyclic transition state would have given $\sqrt{xy}$ = 5.

Unimolecular reactions where $\sqrt{xy}$ = 2.5 and those where $\sqrt{xy}$ = 5 can be interpreted as extremes of a continuum, which reflects the competition of the interconversions depicted in eqs 3 and 4 versus the proton-transfer step represented in eq 1. As expected, there are intermediate cases along this continuum: the metastable ion decomposition of nPrOPh$^{•+}$ ($\sqrt{xy}$ = 4.3),[12] the expulsion of propene from conjugate acid ions of nPrOPh (for which eq 5 depicts a general scheme),[30] or the decomposition of n-propylammonium ions.[27,31]

$$n\text{PrXH}^+ \rightarrow [i\text{Pr}^+ \quad \text{XH}] \overset{-\text{propene}}{\rightarrow} \text{XH}_2^+ \tag{5}$$
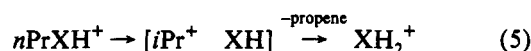
Since n-propyl cation is not predicted to be a stable species,[32] the reaction coordinate for producing an ion–neutral complex can be viewed as an elongation of the sp^3 C–O bond of nPr-OPh$^{•+}$ (or the CX bond of nPrXH$^+$) until the propyl fragment rearranges. If all of the propene expulsions (both from nPrOPh$^{•+}$ and from the even-electron ions represented in eq 5) are viewed as proceeding via the same sort of mechanism, then eq 5 can be used as model for eq 1. This confers advantages from the standpoint of computation, since it becomes possible to use a reasonably large basis set to probe the transition state for the first step of eq 5 when X is a small group like NH$_2$. Here we discuss the position of the electronic energy maximum along this C–N stretching coordinate to model the energy barrier for the bond heterolysis step of eq 1.

Protonated n-propylamine is calculated to have stable *gauche* and *anti* conformers, with the electronic energy of the former nearly 3 kJ mol^{-1} higher than that of the latter. SCF calculations on the first step of eq 5 using the 6-31G** basis set show that the electronic energy of *gauche* nPrNH$_3^+$ rises as the C–N bond is elongated until, somewhere between 2.7 and 2.8 Å, isomerization to an iPr$^+$–ammonia complex takes place and the energy starts to decline. The region near this transition state is shown in Figure 3, with the calculated points for a simple stretch (each corrected for basis set superposition error and computed by optimizing of all other parameters apart from the fixed C–N distance) represented by circles. As the C–N bond stretches the electronic energies of the two rotamers become nearly equal (as can be seen from the confluence of the solid and open circles in Figure 3), even though they remain distinct conformational isomers.

(28) Lemaire, J.; Dimicoli, I.; Botter, R. *Chem. Phys.* **1987**, *115*, 129–142.
(29) Riley, J.; Baer, T. *J. Am. Soc. Mass Spectrom.* **1991**, *2*, 464–469.
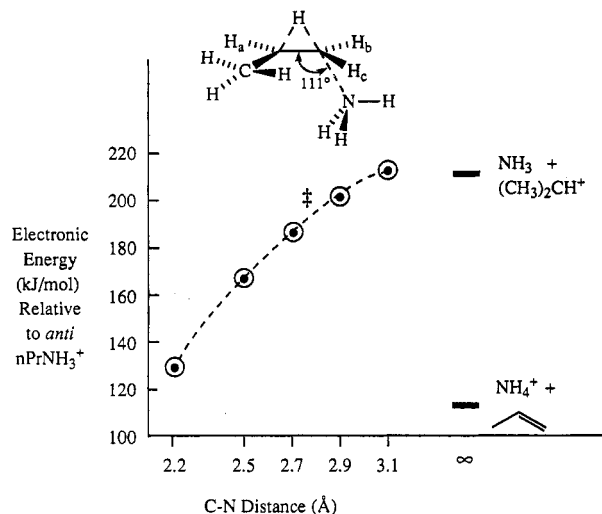(30) (a) Kondrat, R. W.; Morton, T. H. *J. Org. Chem.* **1991**, *56*, 952–957. (b) Kondrat, R. W.; Morton, T. H. *Org. Mass Spectrom.* **1991**, *26*, 410–415.
(31) Bowen, R. D.; Harrison, A. G.; Reiner, E. J. *J. Chem. Soc., Perkin Trans. II* **1988**, 1009–1013.
(32) Koch, W.; Liu, B.; Schleyer, P. v. R. *J. Am. Chem. Soc.* **1989**, *111*, 3479–3480.

Figure 3. SCF potential energy maximum (6-31G**) for hydrogen transposition concomitant with C–N stretch in nPrNH$_3^+$. Position of this transition state is represented by ‡ relative to points calculated for simple C–N stretching of the C–N bond of *gauche* (solid circles) and *anti* (open circles) nPrNH$_3^+$. Electronic energies are corrected for basis set superposition error.

If NH$_3$ is removed from the *gauche* structure after its C–N has been stretched to 3.1 Å, the remaining C$_3$H$_7^+$ fragment rearranges without barrier to isopropyl cation. According to our SCF calculations, though, isomerization of the propyl phenyl group occurs at an energy lower than that needed to stretch the bond to 3 Å. The calculated transition state is drawn in Figure 3, and its position on the distance-energy plot is represented by a double dagger. The electronic energy of this potential energy maximum is only 10 kJ mol^{-1} (corrected for BSSE) below the thermodynamic threshold for producing free isopropyl cation plus ammonia, and it is 90 kJ mol^{-1} above the SCF-calculated thermodynamic threshold for the observed products, propene plus ammonium ion. The nitrogen and migrating hydrogen are not far from being collinear with the carbon terminus ($\angle$HCN = 172°). The nitrogen is 2.6 Å out of the C–C–C plane; the migrating hydrogen is 1.1 Å out of the plane; and the spectator hydrogen (H$_a$, H$_b$, and H$_c$) are very nearly coplanar with the carbons (<0.1 Å out of the C–C–C plane). The hydrogen is almost equidistant between two carbons (1.34 Å from the middle carbon and 1.29 Å from the end carbon, with $\angle$XHX = 63°), and the nitrogen lies in the CHC plane.

Energetically the SCF calculation is consistent with the experimental observation that eq 1 has a barrier much higher than the thermodynamic threshold when R is a primary alkyl group.[14] We conclude that the observed barrier corresponds to the transition state for the bond heterolysis step. For eq 5 this transition state is 52 kJ mol^{-1} higher in energy than the [iPr$^+$ NH$_3$] ion–neutral complex, which has been calculated to be a stable species.[27] In a unimolecular regime, passage from the transition state to [iPr$^+$ NH$_3$] gives a complex with enough internal energy for the isopropyl cation to rotate without hindrance relative to the NH$_3$. We infer that the same picture holds true for decomposition of nPrOPh$^{\bullet+}$ and that an ion–neutral complex is formed that has enough internal energy for the cation to undergo the transpositions depicted in eqs 3 and 4 as well as to rotate freely.

The structure of the transition state, in which H$_a$, H$_b$, and H$_c$ are virtually coplanar with the carbons, erases any structural difference between *gauche* and *anti*. If this is a good description for the transition state for conversion of nPrOPh$^{\bullet+}$ to a [iPr$^+$ PhO$^{\bullet}$] complex, then the slight wavelength dependence of the mass spectra summarized in Table 3 (which may not be significant) can be explained as follows: regardless of the conformation of the neutral precursor, the most energetically

demanding step passes through a transition state whose structure precludes *gauche–anti* conformational isomerism. Therefore the only effect of neutral precursor geometry should be the contribution of its conformational energy to the internal energy of the ion.

Conclusion

The one-color REMPI excitation spectrum of n-propyl phenyl ether in a supersonic jet exhibits three major conformational isomers. The 0,0 absorptions to the first excited state for two of these isomers are close together (17 cm^{-1}) and are assigned to *gauche* and *anti* rotamers of a conformation in which the oxygen, the ring, and two of the alkyl carbons are coplanar. The third conformer has a 0,0 absorption more than 100 cm^{-1} to the blue of the first two and, from *ab initio* estimates of the ordering of conformations, is assigned to another *gauche* geometry.

REMPI mass spectra of these three conformational isomers (and their deuterated analogues) are very nearly the same. Expulsion of propene represents the major fragmentation pathway in the range of laser powers investigated. The seven alkyl hydrogens randomize completely prior to this fragmentation, as has been observed in previous electron impact and field ionization studies.[10] SCF calculations on nPrNH$_3^+$ (as a model for decomposition of nPrOPh$^{\bullet+}$) suggest that hydrogen transfer takes place concomitantly with bond heterolysis, leading to an ion–neutral complex. The potential energy maximum has an electronic energy 90 kJ mol^{-1} above the thermodynamic calculated threshold for product formation, consistent with the high experimental barrier[14] reported for propene expulsion from nPrOPh$^{\bullet+}$.

The experimental data confirm the intermediacy of an ion–neutral complex, which, as would be expected, retains little memory of the geometry of the precursor neutral. The theoretical model supports the conclusion that the barrier to forming the complex is responsible for the high activation energies for decomposition of primary n-alkyl phenyl ether molecular ions. Surmounting this barrier creates complexes with an excess of internal energy, which accounts for the extensive scrambling of the isopropyl hydrogens within [iPr$^+$ PhO$^{\bullet}$] formed by REMPI.

This picture accords with the theory put forth by Winstein and Grunwald for neighboring group participation in solvolysis reactions.[33] Forty-five years ago they proposed that migration of a neighboring group (in the present case a hydrogen) occurs simultaneously with bond heterolysis, a view that is consistent with both the experimental and computational results for the gaseous cations discussed here. If one were to examine other ions, in which nonequivalent neighboring groups compete, they might afford different product distributions from different conformations. Can individual conformers of a precursor neutral be used to create the corresponding molecular ions, in such a fashion that they decompose before reaching conformational equilibrium? That question is the focus of ongoing investigation.

Supplementary Material Available: Power dependence curve for REMPI of nPrOPh, Cartesian coordinates and SCF electronic energies (3-21G//3-21G) for six conformations of neutral nProPh, and SCF vibrational frequencies for the two lowest conformations of nPrOPh and its partially deuterated analogues (9 pages). This material is contained in many libraries on microfiche, immediately follows this article in the microfilm version of the journal, and can be ordered from the ACS; see any current masthead page for ordering information.

(33) Winstein, S.; Grunwald, E. *J. Am. Chem. Soc.* **1948**, *70*, 828–837.